

Cite this: *RSC Pharm.*, 2026, **3**, 564

Reformulating lumefantrine as Flash NanoPrecipitated particles and the impact of incorporation into milk-based formulations on drug solubilisation during digestion

Malinda Salim, ^a Kurt D. Ristroph, ^{b,c} Thomas Eason, ^a Gisela Ramirez,^a Andrew J. Clulow, ^d Robert K. Prud'homme ^e and Ben J. Boyd ^{*a}

Lumefantrine and artemether are currently used as one of the first line therapies for treatment of uncomplicated malaria. However, commercially-available lumefantrine/artemether tablets often result in poor and variable oral bioavailability due to low aqueous solubility of the drugs. To circumvent these issues, consumption of food containing lipids with the lumefantrine/artemether tablet(s) is recommended to increase exposure of the drugs, which brings high variability to the systemic drug exposure. In this study, we investigated the potential use of infant formula as a milk-based lipid formulation to improve the solubilisation of lumefantrine/artemether with controlled fat content, both as a formulation for the two drug substances as well as when co-dosed with lumefantrine after re-formulation into nanoparticles. Time-resolved synchrotron small angle X-ray scattering (SAXS) was used to probe the solubilisation behaviour of the drugs and high-performance liquid chromatography (HPLC) was used to quantify the amount of drugs dissolved during digestion. Findings from these studies suggest that the solubility of artemether in undigested and digested infant formula was greater than 5 fold relative to lumefantrine and that 5 g of fat was not sufficient to completely solubilise a 120 mg lumefantrine dose. When formulated as nanoparticles, there was evidence of slight lumefantrine crystallisation when the highly amorphous drug powder was added to infant formula but digestion did not appear to significantly affect the presence of crystalline lumefantrine. These findings suggest a potential reduced food effect for lumefantrine nanoparticles compared to the crystalline counterpart, further highlighting that lumefantrine nanoparticles may be orally administered in both fasted and fed conditions.

Received 21st October 2025,
Accepted 29th January 2026

DOI: 10.1039/d5pm00294j

rsc.li/RSCPharma

1. Introduction

Lumefantrine and artemether are an artemisinin-based combination therapy that is currently used to treat uncomplicated malaria in adults and children due to *Plasmodium falciparum*.^{1,2} The combination therapy is currently marketed as 60 mg lumefantrine/20 mg artemether tablet under the trade names Riamet® or Coartem®. The recommended fixed-

dose for adults and children 5–15 kg was 480 mg lumefantrine/80 mg artemether and 120 mg lumefantrine/20 mg artemether per dose respectively. It is recommended that the tablets are co-administered with food due to the poorly water-soluble nature of the drugs.^{2,3}

The usefulness of milk and infant formula to improve the oral bioavailability of poorly water-soluble drugs relative to the fasted state relies on the digestion process of the milk-based formulations in the gastrointestinal (GI) tract.^{4,5} Milk and reconstituted infant formula typically contain about 3–5 w/v% fat (of which about 98% are triglycerides)⁶ that are digested into free fatty acids and monoglycerides by endogenous lipases, thereby forming various colloidal liquid crystalline phases in the aqueous environment of the GI tract.⁷ These colloidal structures (such as vesicles, mixed micelles or non-lamellar liquid crystals) have the ability to solubilise poorly water-soluble drugs to keep them in solution prior to absorption,^{8,9} which is especially the case for weakly basic drugs where ion pairing with the liberated fatty acids can enhance solubilisation.¹⁰

^aDrug Delivery, Disposition and Dynamics, Monash Institute of Pharmaceutical Sciences, Monash University (Parkville Campus), 381 Royal Parade, Parkville, VIC 3052, Australia. E-mail: ben.boyd@monash.edu; Fax: +61 3 99039583; Tel: +61 3 99039112

^bDepartment of Agricultural and Biological Engineering, Purdue University, 225 S. University St, West Lafayette, IN 47907, USA

^cDavidson School of Chemical Engineering (by courtesy), Purdue University, 480 Stadium Mall Drive, West Lafayette, IN 47907, USA

^dAustralian Synchrotron, ANSTO, 800 Blackburn Road, Clayton, VIC 3168, Australia

^eDepartment of Chemical and Biological Engineering, Princeton University, Princeton, New Jersey 08540, USA



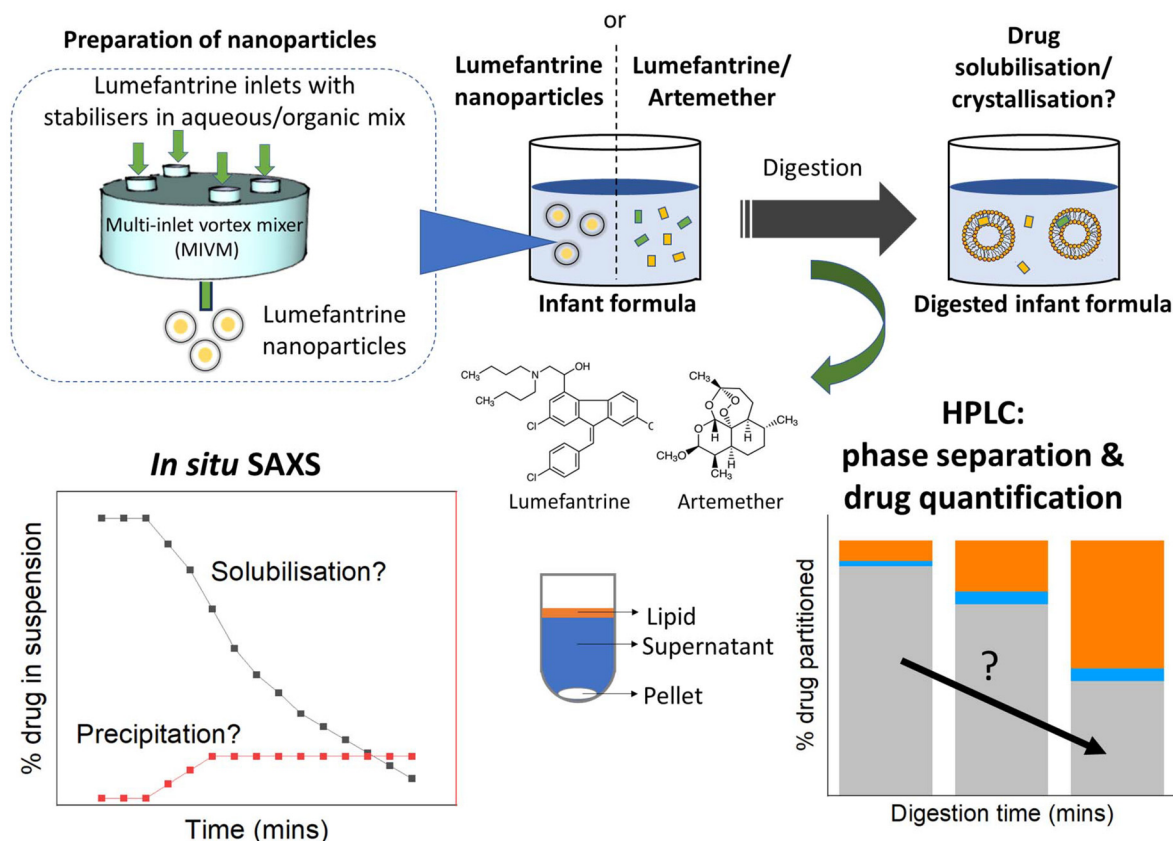


Fig. 1 Schematic illustration of the preparation of lumefantrine nanoparticles using a multi-inlet vortex mixer (MIVM) and the flowchart of this study. Solubilisation or precipitation behaviour of lumefantrine/artemether crystals and lumefantrine nanoparticles in infant formula during digestion was monitored *in situ* using synchrotron small angle X-ray scattering (SAXS). Partitioning of drugs into the digested phases was assessed using HPLC.

However, unlike many basic drugs, previous studies have shown that the solubility of lumefantrine in fed-state simulated small intestinal fluid remained low at a concentration of $14.4 \mu\text{g mL}^{-1}$ in FeSSIF-V2 after 5–6 hours.¹¹ The solubilisation of lumefantrine in milk-based formulations during *in vitro* digestion was also limited¹² although it is currently unclear to what extent the lumefantrine would solubilise given a known amount of fat, and whether the solubilisation of lumefantrine was affected by the presence of artemether and *vice versa*. Consequently, the appropriate volume and fat content required of milk-based formulations to co-administer with a fixed dose of lumefantrine and artemether to provide complete solubilisation of both drugs during digestion remains elusive, and is a hurdle to the development of milk-based excipients for their oral delivery.

This study investigates the solubilisation behaviour of lumefantrine and artemether in infant formula during *in vitro* digestion in single and mixed-dose combinations. The presence of crystalline drugs in suspension was detected using SAXS to monitor *in situ* drug solubilisation during digestion, and HPLC was used to quantify the amount of drug solubilised. In addition to solubilisation of the crystalline active pharmaceutical ingredient (API), this study also aimed to understand the solid-state behaviour of lumefantrine when re-

formulated as nanoparticles and their stability in infant formula during *in vitro* digestion (Fig. 1). These nanoparticles have demonstrated clear advantage over crystalline lumefantrine in enhancing the oral bioavailability *in vivo* when given with water simulating a fasted condition.¹³ However, the effects of food on the oral bioavailability of lumefantrine nanoparticles have not been explored, although *in vitro* drug release in fasted and fed-state simulated small intestinal media (FaSSIF and FeSSIF) showed insignificant differences albeit in the absence of digestion and intake of milk-based formulation.¹³ Findings from these studies will inform the potential of milk-based formulations for oral delivery of lumefantrine/artemether and also serve in adding additional understand of the effects of food intake on the bioavailability of lumefantrine.

2. Materials and methods

2.1 Materials

Lumefantrine (>99%) and artemether (>99%) powders were purchased from Haihang Industry (Jinan, Shandong, China). Halofantrine (>99%) was purchased from GlaxoSmithKline (King of Prussia, PA). Infant formula (brand not disclosed due



to “commercial-in-confidence”) and Riamet® were provided by Medicines for Malaria Venture (MMV). Nutritional information and fatty acid compositions of the infant formula are provided in Tables S1 and S2 respectively in the SI. Each Riamet® tablet contains 120 mg lumefantrine and 20 mg artemether. Sodium taurodeoxycholate hydrate ($\geq 95\%$; Cayman Chemical) and DOPC (1,2-dioleoyl-*sn*-glycero-3-phosphocholine, $\geq 98\%$; Cayman Chemical) were purchased from Sapphire Bioscience (Redfern, NSW, Australia). Quartz and glass capillaries (1.5 mm OD, 80 mm length, 0.01 mm wall thickness) were purchased from Charles Supper Company (Westborough, MA, USA). Trizma® maleate (reagent grade) was purchased from Sigma-Aldrich (St Louis, MO, USA). Calcium chloride dihydrate ($>99\%$) was from Ajax Finechem (Seven Hills, NSW, Australia). Sodium 1-hexanesulfonate ($>98\%$) was purchased from TCI Chemicals (Tokyo, Japan). Sodium chloride ($>99\%$), sodium dihydrogen orthophosphate (98–103%) and methanol (HPLC grade, Labsolv) were purchased from Chem Supply (Gillman, SA, Australia). Dichloromethane ($\geq 99.5\%$) was purchased from Merck (Bayswater, VIC, Australia). Orlistat ($>99\%$, Selleckchem) was purchased from Jomar Life Research (Mulgrave, VIC, Australia). USP grade pancreatin extract was purchased from Southern Biologicals (Nunawading, VIC, Australia). Casein sodium salt was purchased from Sigma-Aldrich (Milwaukee, WI). Pharmaceutical-grade zein was purchased from Flo Chemical Corporation (Ashburnham, MA). AFFINISOL hydroxypropyl methylcellulose acetate succinate (HPMCAS-126) and METHOCEL HPMC E3 were gifts from Dow Chemical Company (Midland, MI).

2.2 Preparation of lumefantrine nanoparticles

Lumefantrine nanoparticles were prepared using Flash NanoPrecipitation and then spray dried to yield a dry powder, as previously described.¹⁴ In brief, to prepare lumefantrine nanoparticles stabilised with HPMCAS, lumefantrine and HPMCAS were dissolved in tetrahydrofuran at 7.5 mg mL⁻¹ and 3.75 mg mL⁻¹, respectively. This stream was fed into a multi-inlet vortex mixer (MIVM) at 16 mL min⁻¹ using a Harvard Apparatus PhD 2000 syringe pump. Three streams of deionised water were also fed into the mixer, each at 48 mL min⁻¹, for a total flow rate of 160 mL min⁻¹ and a final THF volume fraction of 10% (note: a version of this process developed later included NaOH in the deionised water streams to partially neutralise the HPMCAS free acid). Mass of HPMC E3 equivalent to the total mass of the nanoparticles (lumefantrine + HPMCAS) was added to the suspension prior to spray drying (1 : 1 NPs : E3), which was done using a Buchi B-290 lab-scale spray dryer at inlet temperature of 100 °C. The HPMC E3 acts as a matrix former to reduce NP aggregation during drying. For zein/casein-coated NPs, the feed into the MIVM was: one stream of 60/40 v/v ethanol/water containing zein at 6 mg mL⁻¹ and fed at 12 mL min⁻¹; one stream of acetone containing lumefantrine at 6 mg mL⁻¹ and fed at 12 mL min⁻¹; one stream of citrate buffer at pH 7.4 (10 mM sodium citrate, pH adjusted with citric acid) containing sodium caseinate at 1 mg mL⁻¹ and fed at 36 mL min⁻¹; and one stream of citrate buffer

at pH 7.4 fed at 36 mL min⁻¹. The mixer effluent was diluted with additional citrate buffer to decrease the organic solvent volume fraction from 20% to 10%. Zein/casein-coated NPs were dried on the Buchi B-290 at inlet temperature of 100 °C without the addition of additional matrix former.

2.3 Digestion of infant formula containing lumefantrine with or without artemether

Digestion of lumefantrine, artemether or mixtures of lumefantrine and artemether (Table 1) in infant formula was performed using an auto-titrator (pH-STAT apparatus, Metrohm 902 STAT). The drugs were micronised using mortar and pestle and weighed into a glass vial prior to adding 2.5 mL water and 250 μ L 1 M HCl (to mimic a gastric condition). Infant formula was reconstituted using infant simulated small intestinal fluid¹⁵ (iFast; 17.5 mL) and added to the drug suspension and the mixtures were transferred into a jacketed (37 °C) digestion vessel (82 mm height, 78 mm OD, 5–70 mL) operating with a stirrer speed of 750 rpm (speed setting = 6). The infant formula was prepared by mixing 5 mL iFast (sodium taurodeoxycholate/DOPC being 4.7 mM/0.98 mM in Tris) with infant formula powder and Tris buffer up to 20 mL with a target fat content of 3.8 w/v%. The Tris buffer consisted of 50 mM Trizma® maleate, 150 mM NaCl, 5 mM CaCl₂·2H₂O, and 6 mM NaN₃, pH 6.5. Digestion of the infant formula was initiated by injection of 2.25 mL pancreatic lipase (~700 tributyrin unit)¹⁶ and the digestion was performed at pH 6.5, 37 °C by automatic titration of 2 M NaOH using Tiamo version 2.5 software (Metrohm, Herisau, Switzerland).

Due to the low drug loading (section 2.2) and limited powders available, digestion of lumefantrine nanoparticles with infant formula was performed in a small volume *in vitro* setup described previously.¹⁷ Powders were weighed to 20 mg equivalent lumefantrine and added to 913 μ L water (or 830 μ L water and 83 μ L 1 M HCl in water to mimic a gastric condition) and 6.75 mL infant formula (reconstituted using iFast) in a 20 mL glass vial. The pH of the formulation was adjusted to 6.5 and digestion was initiated by addition of 750 μ L pancreatic lipase during digestion, the pH was maintained at 6.5 by automatic titration of 0.2 M NaOH.

2.4 Solubilisation of lumefantrine and artemether during digestion

Solubilisation of lumefantrine and artemether in infant formula during digestion was investigated by quantifying the amount of drug partitioned into the aqueous supernatant layer and the lipid layer after ultracentrifugation. Samples

Table 1 Amount of lumefantrine/artemether mix and their corresponding ratios tested in our studies

| Ratio of lumefantrine : artemether (w/w) | Lumefantrine (mg) | Artemether (mg) |
|--|-------------------|-----------------|
| 1 : 1 | 60 | 60 |
| 1 : 4 | 30 | 120 |
| 4 : 1 | 120 | 30 |



(200 μL) before and during digestion were collected and 4 μg of orlistat (2 mg mL^{-1} in methanol) was added to inhibit the lipolysis. The samples were subsequently ultracentrifuged at 329 177g for 20 min at 37 °C (Optima MAX-TL, TLA-100 rotor) after which the upper lipid layer (that consists of lamellar calcium soaps and non-lamellar liquid crystalline structures), the aqueous supernatant layer (mixed micelles) and the pelleted layer (undissolved drug) were separated and stored at -20 °C prior to drug separation and quantification using HPLC.

2.5 Solubility of lumefantrine and artemether in infant formula and digested infant formula

Excess lumefantrine and artemether were separately incubated with freshly reconstituted infant formula (3.8 w/v% fat) and digested blank infant formula (collected after 60 min digestion, pH 6.5) at 37 °C. The pH of the samples was monitored throughout incubation and adjusted as necessary to 6.5. The collected samples (200 μL) were incubated over 48 h and subsequently ultracentrifuged using parameters described in section 2.4. The aqueous supernatant layer and the lipid layer were collected and stored at -20 °C prior to HPLC.

2.6 Small angle X-ray scattering

2.6.1 Static capillary. Lumefantrine, artemether, crushed Riamet® tablet and lumefantrine nanoparticles were filled into glass capillaries. The capillary was placed in the X-ray beam (wavelength $\lambda = 0.954 \text{ \AA}$, photon energy = 13 keV) at the SAXS/WAXS beamline at the Australian Synchrotron, ANSTO.¹⁸ The acquisition time was 1 s and the sample-to-detector distance for capillaries and the flow-through configuration in section 2.6.2 was about 560 mm to cover $0.04 < q < 1.8 \text{ \AA}^{-1}$ where q (scattering vector) = $(4\pi/\lambda)\sin\theta$; with 2θ being the scattering angle. Raw data from the two-dimensional SAXS pattern (acquired using a Pilatus 1 M detector) was reduced to the scattering function $I(q)$ vs. q using an in-house developed software package Scatterbrain version 2.71.

2.6.2 Flow-through digestion. The pH-STAT digestion apparatus and the small volume *in vitro* digestion apparatus were interfaced to the SAXS/WAXS beamline at the Australian Synchrotron, ANSTO.¹⁸ In the former, samples were circulated from the digestion vessel through silicone tubing (2 mm ID, 4 mm OD) to a free-standing quartz capillary (that was placed on the X-ray beam; wavelength = 0.954 \AA , photon energy = 13 keV) using a peristaltic pump (Masterflex™ C/L variable-speed tubing pump) operating at approximately 10 mL min^{-1} . The approximate total volume in circulation was 2.5 mL. Digestion was initiated *via* remote injection of pancreatic lipase. Acquisition time was 5 s every 20 s (*i.e.* 15 s delay in measurements).

A “push-pull” approach was used for the small volume *in vitro* digestion setup described previously¹⁷ where samples (<800 μL) were aspirated (“pulled”) from the glass vial through silicone tubing (2 mm ID, 4 mm OD) to the free-standing quartz capillary and “pushed” back into the vial. Acquisition time was 5 s every 15 s.

2.7 High performance liquid chromatography

Lumefantrine and artemether were extracted from the collected lipid layer, aqueous supernatant layer and pellet layer prior to gradient elution separation using a reversed phase C18 HPLC column (Waters Symmetry, 4.6 mm \times 75 mm, 3.5 μm , 100 \AA). For lumefantrine, dichloromethane (800 μL containing halofantrine as internal standard) or methanol (200 μL) + dichloromethane (800 μL containing halofantrine as internal standard) was added to the aqueous supernatant and the lipid/pellet layer respectively and the mixtures were centrifuged for 10 min at 16 163g to remove precipitated proteins. The samples were subsequently diluted in 35 v/v% mobile phase A (23 mM sodium dihydrogen phosphate and 30 mM sodium hexanesulfonate in water, pH 2.3) + 65 v/v% mobile phase B (methanol). Meanwhile, artemether was extracted from the aqueous supernatant layer, the lipid layer and the pellet layer using methanol that contained halofantrine as internal standard. Separation of lumefantrine and artemether was performed using the same conditions: 65 v/v% to 90 v/v% B over 10 min, hold at 90 v/v% for 1 min followed by 4.5 min equilibration at 65 v/v%. The flowrate was set to 1 mL min^{-1} , injection volume was 20 μL , temperature of the column was 35 °C and the drugs were detected using a UV detector (255 nm for lumefantrine/halofantrine and 220 nm for artemether). The retention time (in the order of elution) was about 6.5 min for artemether, 7.5 min for halofantrine and 8.4 min for lumefantrine.

3. Results and discussion

3.1 Solid-state behaviour of lumefantrine and artemether

Sharp Bragg peaks observed from the characteristic X-ray scattering patterns for lumefantrine, artemether and Riamet® in Fig. 2 indicate that the drugs are crystalline prior to suspension. The individual peak positions are summarised in Table S3 in the SI. While only one polymorphic form for lumefantrine has been identified,¹⁹ artemether exists as two polymorphs (polymorph A and B)²⁰ and the artemether used in this study was form B. Characteristic peaks for lumefantrine and artemether were taken to be $q = 1.64$ and 1.26 \AA^{-1} respectively, which were used to monitor the drug solubilisation during *in vitro* digestion.

3.2 Effects of artemether on the solubilisation of lumefantrine during *in vitro* digestion and *vice versa*

Solubilisation behaviour of lumefantrine, both in the presence and absence of artemether, in infant formula during digestion was monitored *in situ* using synchrotron SAXS. An example scattering pattern is shown in Fig. 3a, where the characteristic Bragg peaks of lumefantrine and artemether were tracked over time during dispersion and digestion. The integrated areas of these characteristic peaks are presented in Fig. 3b and c respectively.

Fig. 3b confirms that solubilisation of lumefantrine was not affected by the presence of artemether (unlike other combination drug therapies such as lopinavir/ritonavir²¹ and arte-



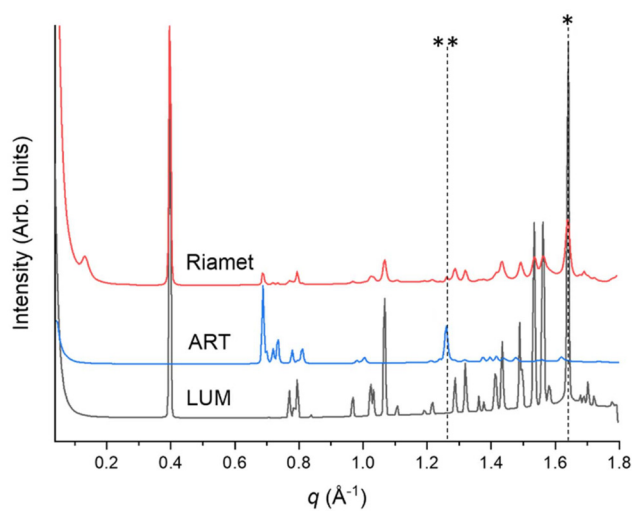


Fig. 2 X-ray scattering patterns of lumefantrine powder (LUM), artemether powder (ART) and crushed Riamet® tablet (Riamet). Asterisk (*) and double asterisks (**) point to the peak positions for lumefantrine ($q = 1.64 \text{ \AA}^{-1}$) and artemether ($q = 1.26 \text{ \AA}^{-1}$) respectively that were used to monitor drug solubilisation during *in vitro* digestion.

methem/ferroquine²²) and that the peak area for lumefantrine decreased very slightly during digestion of infant formula in the presence of artemether at 1 : 1, 1 : 4 and 4 : 1 lumefantrine : artemether ratio. The amount of fatty acids released during digestion at pH 6.5 was also comparable (Fig. S1). Similarly, the solubilisation of artemether during digestion in infant formula was independent to lumefantrine (Fig. 3b). However, due to its lower lipophilicity ($\text{clog } D_{7.4} = 2.80$ compared to 7.34 for lumefantrine)¹¹ and melting point ($87 \text{ }^\circ\text{C}$ vs. $129 \text{ }^\circ\text{C}$),¹¹ artemether was highly soluble in the undigested infant formula and a significant decrease in peak area was observed during dispersion (Fig. 3c). The higher affinity of artemether towards fat globules compared to lumefantrine was also supported by its 5-fold higher drug solubility in the undigested infant formula as was shown in Table 2 ($53.5 \pm 1.5 \text{ mg g}^{-1}$ fat for artemether vs. $10.1 \pm 3.8 \text{ mg g}^{-1}$ fat for lumefantrine).

Injection of pancreatic lipase further accelerated the solubilisation of artemether and complete disappearance of the drug crystals was attained after digestion (Fig. 3b). Quantification of the partitioned artemether into the lipid and aqueous supernatant layers by HPLC after 60 min digestion corroborated findings from SAXS, and complete drug solubilisation was observed even when the dose was increased to 120 mg (Fig. S2). This indicates that the solubility of artemether in digested infant formula could exceed 180 mg g^{-1} of fat. The high capacity of digested infant formula to solubilise artemether was also reflected from the solubility measurements (Table 2) but it is worth noting that the drug suspension underwent discoloration during incubation at $37 \text{ }^\circ\text{C}$ and the presence of a small degradant peak was also observed in the undigested infant formula samples (Fig. S3). Nevertheless, the results confirmed that artemether was highly soluble in infant formula and a small volume intake of infant formula (~about

12 mL) was sufficient to solubilise a single dose of artemether for children and adults. The extent and kinetics of artemether solubilisation in the small intestine is therefore not a limiting factor to its absorption.

By comparison, given the poor aqueous solubility of lumefantrine ($<0.05 \text{ } \mu\text{g mL}^{-1}$ in phosphate buffered saline, pH 7.4 mg mL^{-1} (ref. 11) compared to $109 \text{ } \mu\text{g mL}^{-1}$ for artemether),¹¹ the fraction of dose absorbed for lumefantrine was as low as $<10\%$ in the fasted conditions.²³ Consumption of lumefantrine and artemether with food containing lipids, such as milk, has therefore been recommended by World Health Organization (WHO)² and the prescribing information for Riamet® or Coartem®.³ However, the quantity of fat, volume, and types of milk (including bovine, soya or human milk) required to be orally administered per dose of lumefantrine is not stipulated in the prescribing information and remains a possible variable in determining the oral bioavailability of lumefantrine in the fed state. Additionally, there is still no agreement on how much fat is required to increase the exposure of lumefantrine. For example, Mwebaza *et al.* observed a 2.7-fold improvement in $\text{AUC}_{(0-48)}$ when administering 480 mg lumefantrine with 200 mL of milk,²⁴ but only 10 mL of soya milk was required to obtain the equivalent fold increase in AUC for the same dose.²⁵ In a similar evaluation, an advanced compartmental absorption and transit (ACAT) model in GastroPlus with 10 mL soya milk predicted that the fraction of lumefantrine absorbed was only $\sim 35\%$ in infants $>5 \text{ kg}$.²⁶ It is therefore likely that a larger volume of milk could be required to increase the oral bioavailability of lumefantrine.

It is accepted that co-administration of lipids with poorly water-soluble drugs can serve to enhance the solubilisation of drugs by providing colloidal structures formed by the self-assembly of lipid digestion products (fatty acids and monoglycerides) into which the drugs have enhanced solubility compared to the lipid-free environment.⁸ In the case of weakly basic drugs, the ability to also ion pair with fatty acids to form non-crystalline precipitates can contribute to further enhance solubilisation during digestion¹⁰ However, the solubilisation of lumefantrine in digesting milk is limited.¹² Using both synchrotron SAXS and low frequency Raman scattering, we have previously shown very limited solubilisation of lumefantrine in milk, while a slight drug solubilisation was observed in infant formula.¹² These results suggest that infant formula may be better suited as a formulation to co-administer lumefantrine compared to milk. Table 2 shows that the solubility of lumefantrine in digested infant formula was higher than in undigested infant formula, suggesting that digestion would drive enhanced solubilisation. The amount of lumefantrine soluble in the digested infant formula was estimated to be $39.3 \pm 1.4 \text{ mg g}^{-1}$. This value may be an overestimate, as a portion of the undissolved lumefantrine in digested infant formula did not sediment when ultracentrifuged and instead moved to the creamed lipid layer (Fig. 4). This observation suggests that ultracentrifugation did not generate sufficient force to dewet all of the lumefantrine particles, preventing a portion of the undissolved drug particles from sedimenting into the



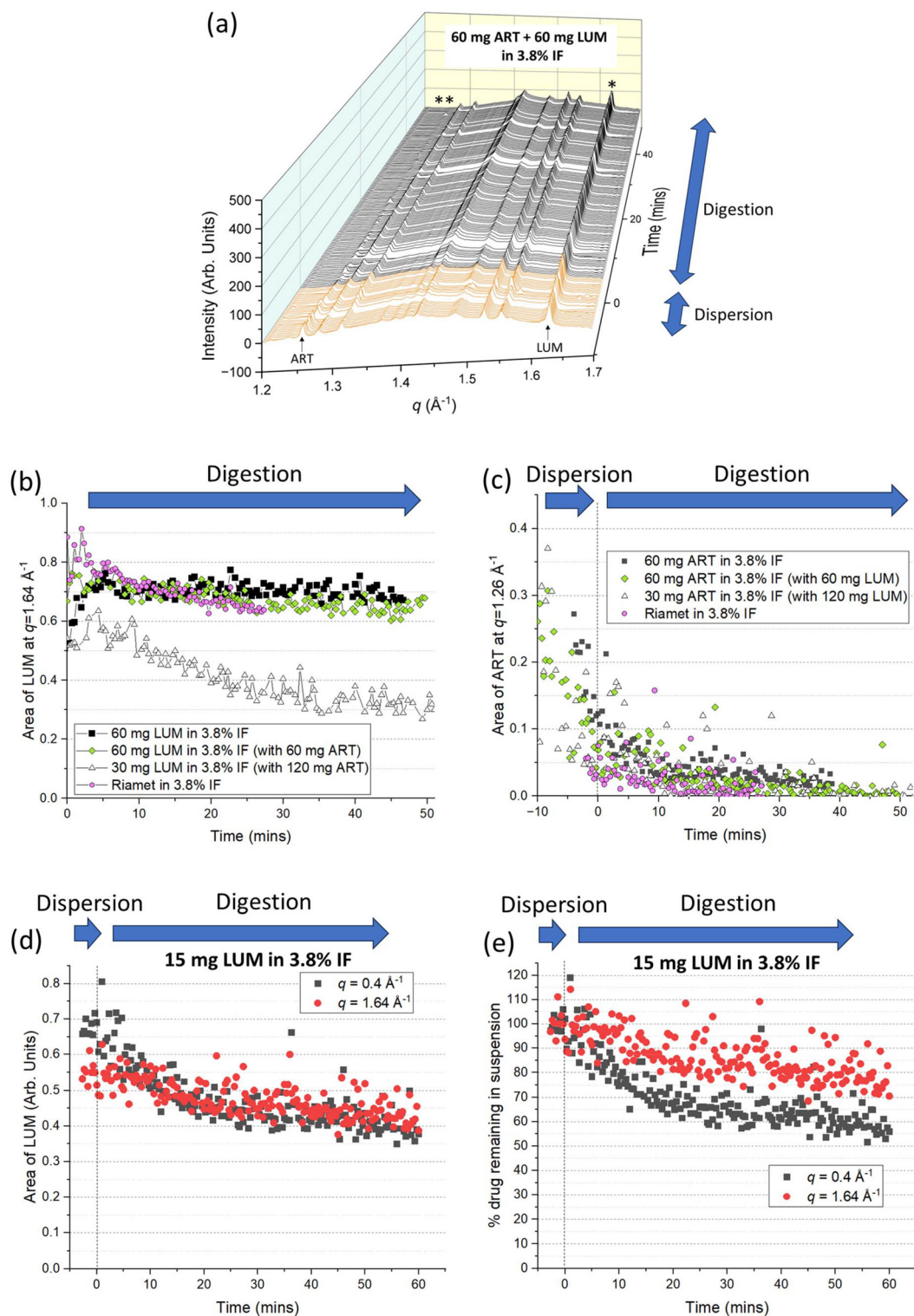


Fig. 3 (a) Example X-ray scattering pattern of lumefantrine and artemether during dispersion (time < 0 min) and digestion (time > 0 min) of 3.8 w/v% infant formula (IF). Pancreatic lipase was injected at 0 min. Changes in the characteristic peak area for lumefantrine ($q = 1.64 \text{ \AA}^{-1}$) and artemether ($q = 1.26 \text{ \AA}^{-1}$) in the presence or absence of its partner drug are shown in panel (b) and (c) respectively. (d) Changes in the characteristic peak area of lumefantrine (15 mg) during dispersion and digestion in 3.8 w/v% IF at $q = 1.64 \text{ \AA}^{-1}$ to demonstrate incomplete drug solubilisation after digestion. Peak area at another major scattering peak position at $q = 0.4 \text{ \AA}^{-1}$ was included for comparison. (e) The corresponding percentage of drug remaining in suspension.



Table 2 Solubility of lumefantrine and artemether in infant formula and digested infant formula at pH 6.5, 37 °C determined using HPLC ($n = 3 \pm \text{SD}$)

| Drug | Infant formula | | Digested infant formula | |
|--------------|------------------------|-------------------------|-------------------------|--------------------------|
| | mg mL ⁻¹ | mg g ⁻¹ fat | mg mL ⁻¹ | mg g ⁻¹ fat |
| Lumefantrine | 0.4 ± 0.1 ^a | 10.1 ± 3.8 ^a | 1.5 ± 0.1 ^b | 39.3 ± 1.4 ^b |
| Artemether | 2.0 ± 0.1 ^c | 53.5 ± 1.5 ^c | 7.2 ± 0.3 ^d | 188.4 ± 7.1 ^d |

The different superscript letters indicate statistically significant differences (p value < 0.05) between infant formula and digested infant formula for each drug (lumefantrine: a, b; artemether: c, d) based on paired two-tailed t -tests performed in GraphPad Prism version 10.4.1.

pellet. As a consequence, some crystalline lumefantrine was collected with the aqueous and lipid phases and was thus quantified as solubilised drug. This phenomenon has also been observed for ritonavir.²¹

This issue highlights the challenges in phase separation and drug quantification using HPLC in such studies, an issue that is absent when using *in situ* SAXS observations of changes in the amount of crystalline drug present during digestion. Thus, the solubilisation capacity of lumefantrine in digested infant formula is better estimated based on the SAXS data. Fig. 3d and e shows that in the absence of artemether and with limited concentration of bile salt, incomplete solubilisation of lumefantrine was evident for 15 mg drug in 0.67 g infant formula fat. These findings suggest that the solubilisation capacity of lumefantrine was <23 mg g⁻¹ fat hence

>140 mL of 3.8 w/v% fat infant formula would be required to solubilise a 120 mg dose although the level could vary depending on concentrations of bile salts.

The minimum amount of fat (and the corresponding infant formula powder) required to solubilise a given dose of lumefantrine can be potentially used to inform future development of infant formula-based lipid formulations for lumefantrine and artemether. Similarly, on the basis of minimising the variable intake of lipids and their impact on oral bioavailability of poorly water-soluble drugs, indicating the minimum volume, amount, and types of lipids per dose of API (even for the existing tablet form within prescribing information) can be a potential way to mitigate the risks of under- or over-dosing in paediatric patients.

3.3 Re-formulating lumefantrine as nanoparticles and the impact on drug solubilisation

The low and variable oral bioavailability of lumefantrine has subsequently guided the re-formulation of lumefantrine towards amorphous dosage forms.^{13,27,28} Co-authors on this paper recently reported that hydroxypropyl methylcellulose acetate succinate (HPMCAS)-stabilised lumefantrine nanoparticles prepared using the Flash NanoPrecipitation (FNP) technique²⁹ (schematic in Fig. 1) provided a 4.8 fold increase in oral bioavailability compared to crystalline lumefantrine in the fasted state.¹³ The nanoparticles also showed rapid dissolution in FaSSIF and FeSSIF *in vitro* with no significant differences observed over a period of 4 weeks.¹³ However, the dissolution of lumefantrine nanoparticles in milk-based formulations as vehicles for drug administration in paediatric

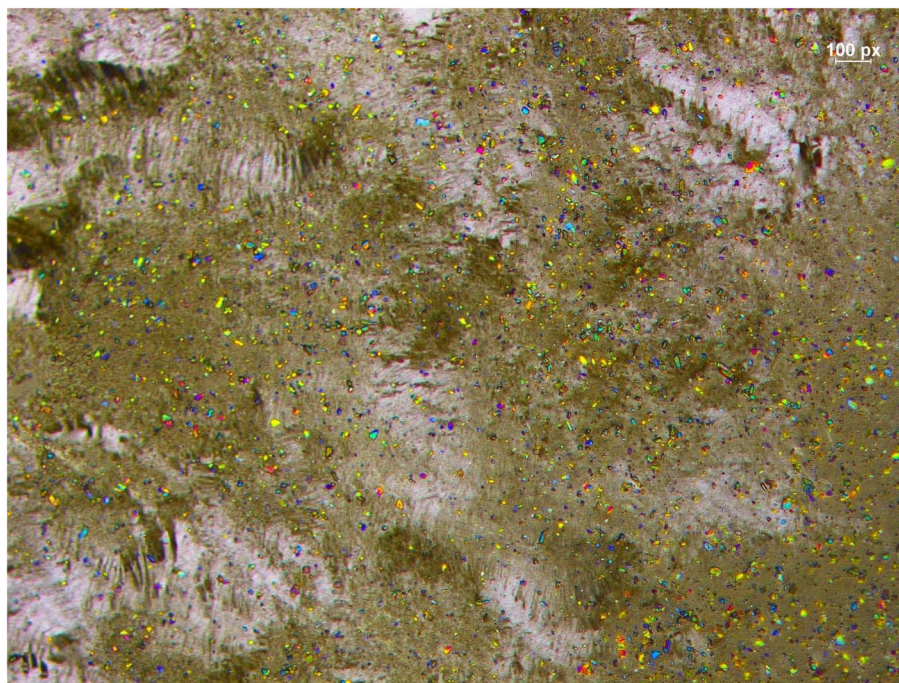


Fig. 4 Polarised microscopy image of the upper lipid layer of digested lumefantrine in infant formula separated by ultracentrifugation which show distributions of lumefantrine crystals in the lipid layer. Scalebar: 100 px = 120 μm .



populations and the effects of different stabilisers has not been explored but may offer an option to further enhance drug solubilisation and reduced dose of drug and excipients to achieve sufficient exposure.

Fig. 5b shows that the 'as prepared' lumefantrine nanoparticles stabilised with HPMCAS and zein (particle size distributions in Fig. 5a) were not completely amorphous (despite the significant increase in oral bioavailability for HPMCAS described above) as characteristic Bragg peaks indicative of crystalline lumefantrine at $q = 0.4$ and 1.64 \AA^{-1} were observed. The intensity of Bragg peaks was lower in HPMCAS- compared to zein-stabilised nanoparticles.

When studying these systems using *in situ* SAXS during digestion, it is a different paradigm to studies starting with crystalline drug – the 'ideal' scenario is that drug is initially amorphous so the integrated area under the crystalline peaks is

low or below detection, and during digestion it should stay low; if crystallisation occurs, the integrated peak area will start to increase, and significant crystallisation will result in a significant increase in the peak area. When dispersed in Tris buffer and Tris buffer containing bile salts (iFast), the HPMCAS-stabilised lumefantrine nanoparticles stayed relatively stable and no significant increase in crystallisation occurred. However, when the HPMCAS-stabilised nanoparticles were dispersed in infant formula alone and digested (Fig. 5c), a slight increase in the peak area for lumefantrine was observed, compared to buffer and bile salt media (iFast). Crystallisation of the lumefantrine in infant formula may be caused by the increased drug dissolution by the fat globules and/or presence of "impurities" that can act as nucleation sites for crystallisation. The process of crystallisation also appeared to be slightly accelerated during the digestion of infant formula (Fig. 5c).

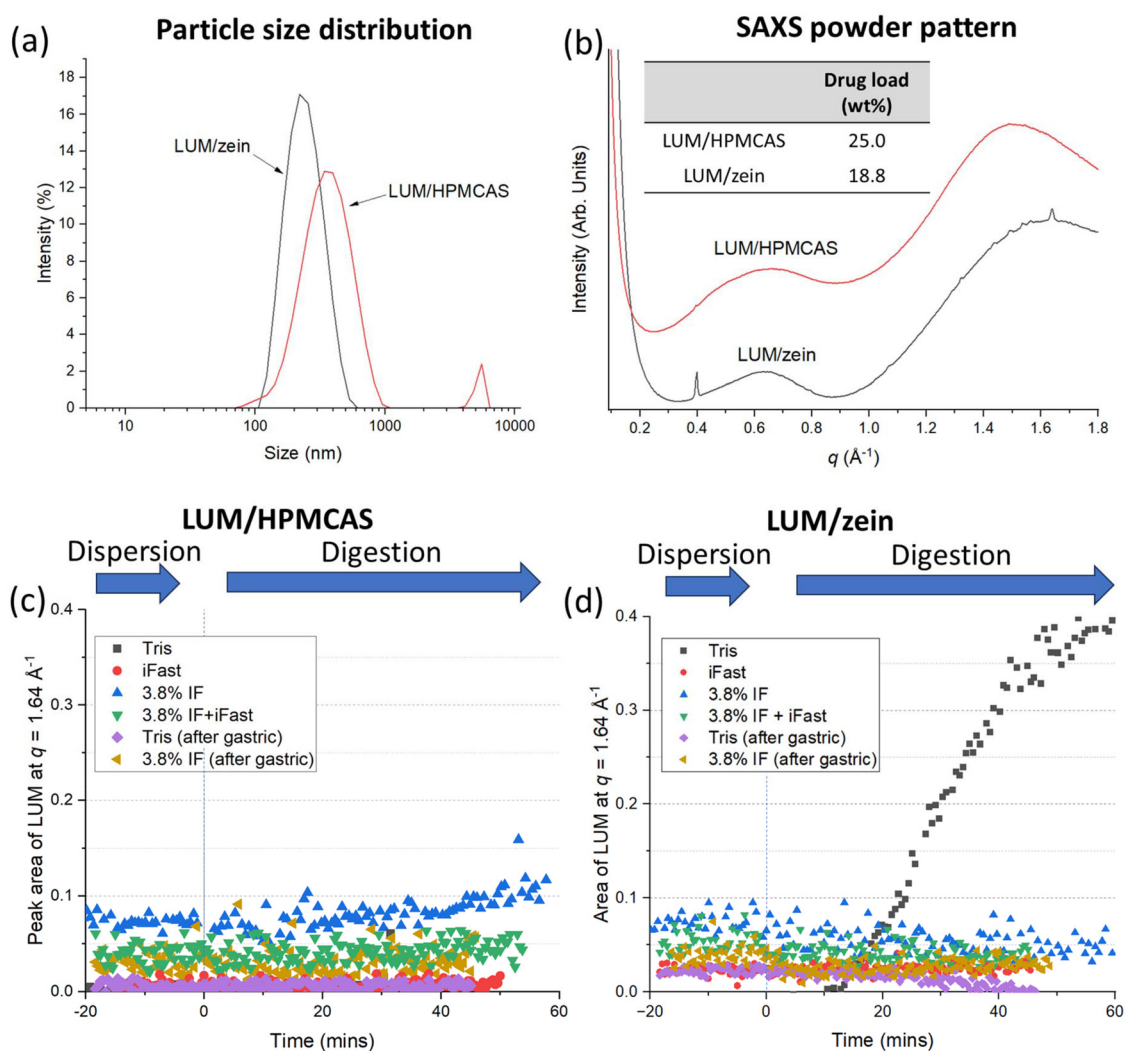


Fig. 5 (a) Particle size distributions of dispersed HPMCAS- and zein-stabilised lumefantrine nanoparticles with z-average of approximately 380 nm (polydispersity index = 0.3) and 230 nm (polydispersity index = 0.1) respectively. (b) X-ray scattering pattern of the lumefantrine nanoparticles after spray-drying at 100 °C with drug content tabulated in inset. Area of the integrated characteristic peak for lumefantrine during dispersion and digestion of re-dispersed (c) HPMCAS and (d) zein-stabilised lumefantrine nanoparticles in various media.



Similarly, in the case of zein-stabilised lumefantrine nanoparticles, there was little change in the low amount of crystallised material in most of the media including infant formula during digestion (Fig. 5d). However, interestingly, a rapid and significant increase in the lumefantrine Bragg peak was observed about 10 minutes after injection of pancreatic lipase to the dispersed nanoparticles in Tris buffer (Fig. 5d). Because zein can be hydrolysed by proteases in the pancreatin,³⁰ it is hypothesised that this onset of crystallisation was caused by the release of encapsulated lumefantrine following proteolysis which, in the absence of infant formula and bile salts, could not be subsequently dissolved. It is worth mentioning that pre-treatment of the formulation in the gastric phase (Tris, after gastric; Fig. 5d) involved only lowering of the pH and did not provide a mechanism for digestion. The role of pepsin on drug crystallisation therefore requires further investigation, as is the case for the impact of enzymes on other digestible stabilisers during product development. This study suggests that co-administration of zein/lumefantrine nanoparticles with infant formula could present a significant advantage in this instance as the digested lipid products would assist in re-solubilisation of the precipitated drug crystals. Overall, findings from this study also highlight the importance of selecting excipients when formulating nanoparticles for oral administration, given the presence of complex environment and enzymatic processes in the gastrointestinal tract.

4. Conclusions

Understanding the solubilisation behaviour of lumefantrine and artemether in infant formula during digestion is key to the development of milk-based formulations for artemisinin-based combination therapy and guidance to intake of infant formula following oral administration of the fixed-dose combination tablets. Our studies conclude that solubilisation of lumefantrine and artemether was enhanced by digestion of infant formula. The amount of fat in infant formula required to solubilise artemether was significantly lower than lumefantrine and it is estimated that >5 g of fat was required to fully solubilise a 120 mg dose of lumefantrine. Lumefantrine nanoparticles stabilised with HPMCAS had lower initial drug crystallinity compared to zein-stabilised particles. Formulating lumefantrine as nanoparticles was beneficial in preventing crystallisation of drug during digestion, and keeping drug in a non-crystalline state, which was enhanced by the presence of infant formula in the case of zein-stabilised nanoparticles but slightly increased crystallisation of drug in the case of HPMCAS-stabilised nanoparticles. *In vivo* performance of lumefantrine nanoparticles in the presence of infant formula has not been confirmed although it is anticipated that the exposure of lumefantrine may not be significantly affected due to the low level of drug crystallisation observed *in vitro* compared to crystalline lumefantrine.

Author contributions

Conceptualisation: B. J. B., R. K. P., K. D. R. Methodology: M. S., G. R., A. J. C., B. J. B. Formal analysis: M. S., G. R. Funding acquisition: B. J. B. Investigation: M. S., G. R., T. E., A. J. C., B. J. B., K. D. R. Project administration: B. J. B. Resources: B. J. B., R. K. P., K. D. R. Supervision: B. J. B. Writing – original draft: M. S., B. J. B. Writing – review and editing: M. S., B. J. B., K. D. R.

Conflicts of interest

The authors declare no conflicts of interest.

Data availability

The data supporting this article have been included as part of the supplementary information. Supplementary information: Table S1 = Nutritional information of the infant formula used in this study. Table S2 = Fatty acids composition of the infant formula after digestion by pancreatic lipase. Table 3 = Bragg peak positions for lumefantrine, artemether and Riamet®. Fig. S1 = Titrated (ionised) fatty acids during digestion of infant formula containing lumefantrine and artemether. Fig. S2 = Partitioning of artemether in phases separated by ultracentrifugation during digestion of infant formula. Fig. S3 = HPLC chromatogram of artemether showing the presence of a degradant. See DOI: <https://doi.org/10.1039/d5pm00294j>.

Acknowledgements

This work was funded by the Bill and Melinda Gates Foundation under Investment IDs OPP1160404 and OPP1150755. Funding is also acknowledged from the Australian Research Council under the Discovery Projects scheme DP160102906. A. J. C. is the recipient of a Discovery Early Career Research Award (DE190100531). K. D. R. was the recipient of a United States National Science Foundation Graduate Research Fellowship (DGE-1656466). The SAXS experiments for this work were conducted on the SAXS/WAXS beamline of the Australian Synchrotron, part of ANSTO.

References

- 1 WHO, World malaria report, <https://www.who.int/teams/global-malaria-programme/reports/world-malaria-report-2022>.
- 2 WHO, *Guidelines for the treatment of malaria*, 3rd edn, 2015.
- 3 Novartis, *Coartem full prescribing information*, 2019.
- 4 B. J. Boyd, M. Salim, A. J. Clulow, G. Ramirez, A. C. Pham and A. Hawley, *J. Controlled Release*, 2018, **292**, 13–17.
- 5 M. Salim, T. Eason and B. J. Boyd, *Adv. Drug Delivery Rev.*, 2022, **183**, 114139.



- 6 P. F. Fox and P. L. McSweeney, *Advanced dairy chemistry volume 2: lipids*, Springer Science & Business Media, 2007.
- 7 A. J. Clulow, M. Salim, A. Hawley and B. J. Boyd, *Chem. Phys. Lipids*, 2018, **211**, 107–116.
- 8 G. A. Kossena, B. J. Boyd, C. J. H. Porter and W. N. Charman, *J. Pharm. Sci.*, 2003, **92**, 634–648.
- 9 K. Kleberg, F. Jacobsen, D. G. Fatouros and A. Müllertz, *J. Pharm. Sci.*, 2010, **99**, 3522–3532.
- 10 J. Khan, T. Rades and B. J. Boyd, *Mol. Pharm.*, 2016, **13**, 3783–3793.
- 11 S. A. Charman, A. Andreu, H. Barker, S. Blundell, A. Campbell, M. Campbell, G. Chen, F. C. K. Chiu, E. Crighton, K. Katneni, J. Morizzi, R. Patil, T. Pham, E. Ryan, J. Saunders, D. M. Shackelford, K. L. White, L. Almond, M. Dickins, D. A. Smith, J. J. Moehrle, J. N. Burrows and N. Abla, *Malar. J.*, 2020, **19**, 1.
- 12 M. Salim, S. J. Fraser-Miller, K. r. Bērziņš, J. J. Sutton, G. Ramirez, A. J. Clulow, A. Hawley, S. Beilles, K. C. Gordon and B. J. Boyd, *Mol. Pharm.*, 2020, **17**, 885–899.
- 13 M. Armstrong, L. Wang, K. Ristroph, C. Tian, J. Yang, L. Ma, S. Panmai, D. Zhang, K. Nagapudi and R. K. Prud'homme, *J. Pharm. Sci.*, 2023, **112**, 2267–2275.
- 14 J. Feng, Y. Zhang, S. A. McManus, R. Qian, K. D. Ristroph, H. Ramachandrani, K. Gong, C. E. White, A. Rawal and R. K. Prud'homme, *Soft Matter*, 2019, **15**, 2400–2410.
- 15 D. Kamstrup, R. Berthelsen, P. J. Sassene, A. Selen and A. Müllertz, *AAPS PharmSciTech*, 2017, **18**, 317–329.
- 16 M. Salim, A. K. H. MacGibbon, C. J. Nowell, A. J. Clulow and B. J. Boyd, *Colloids Interfaces*, 2023, **7**, 56.
- 17 N. F. Khan, M. Salim, S. Y. Binte Abu Bakar, K. Ristroph, R. K. Prud'homme, A. Hawley, B. J. Boyd and A. J. Clulow, *Int. J. Pharm.: X*, 2022, **4**, 100113.
- 18 N. M. Kirby, S. T. Mudie, A. M. Hawley, D. J. Cookson, H. D. T. Mertens, N. Cowieson and V. Samardzic-Boban, *J. Appl. Crystallogr.*, 2013, **46**, 1670–1680.
- 19 Novartis, *NDA 22-268, Chemistry review, Coartem (artemether/lumefantrine) tablets, 20 mg/120 mg*, 2009.
- 20 D. Z. L. Ng, A. Z. Nelson, G. Ward, D. Lai, P. S. Doyle and S. A. Khan, *Pharm. Res.*, 2022, **39**, 411–421.
- 21 M. Salim, G. Ramirez, A. J. Clulow, A. Hawley and B. J. Boyd, *Mol. Pharm.*, 2023, **20**, 2256–2265.
- 22 M. Salim, J. Khan, G. Ramirez, M. Murshed, A. J. Clulow, A. Hawley, H. Ramachandrani, S. Beilles and B. J. Boyd, *Mol. Pharm.*, 2019, **16**, 1658–1668.
- 23 N. J. White, M. van Vugt and F. D. Ezzet, *Clin. Pharmacokinet.*, 1999, **37**, 105–125.
- 24 N. Mwebaza, M. Jerling, L. L. Gustafsson, C. Obua, P. Waako, M. Mahindi, M. Ntale, O. Beck and U. Hellgren, *Basic Clin. Pharmacol. Toxicol.*, 2013, **113**, 66–72.
- 25 E. A. Ashley, K. Stepniewska, N. Lindegårdh, A. Annerberg, A. Kham, A. Brockman, P. Singhasivanon, N. J. White and F. Nosten, *Trop. Med. Int. Health*, 2007, **12**, 195–200.
- 26 W. Lin, T. Heimbach and H. He, *Formulation-dependent pediatric physiologically based pharmacokinetic (PPBPK) modeling to aid drug development*, Novartis, 2016.
- 27 D. Liu, S. Li, D. S. Jones and G. P. Andrews, *Br. J. Pharm.*, 2022, **7**, S1–S2.
- 28 T. N. Hiew, D. Y. Zemlyanov and L. S. Taylor, *Mol. Pharm.*, 2021, **19**, 392–413.
- 29 K. D. Ristroph, N. M. Pinkerton, C. E. Markwalter, S. M. D'Addio, M. E. Gindy and R. F. Pagels, *Adv. Drug Delivery Rev.*, 2025, **227**, 115700.
- 30 P. Hurtado-López and S. Murdan, *J. Microencapsulation*, 2006, **23**, 303–314.

